

# Fidelity of the near resonant quantum kicked rotor

Probst B, Dubertrand R and Wimberger S

Institute for Theoretical Physics and Center for Quantum Dynamics, University of Heidelberg, Philosophenweg 19, D-69120 Heidelberg

**Abstract.** We present a perturbative result for the temporal evolution of the fidelity of the quantum kicked rotor, i.e. the overlap of the same initial state evolved with two slightly different kicking strengths, for kicking periods close to a principal quantum resonance. Based on a pendulum approximation we describe the fidelity for rotational orbits in the pseudo-classical phase space of a corresponding classical map. Our results are compared to numerical simulations indicating the range of applicability of our analytical approximation.

PACS numbers: 03.65.Sq, 05.60.Gg, 03.75.Dg, 37.10.Vz

## 1. Introduction

In classical mechanics chaos can be defined using the stability of a trajectory. Consider two neighbouring phase space points, the distance of their orbits in the phase space will grow exponentially in time for a generic chaotic system. Such an approach is bound to fail in a quantum mechanical treatment as the time evolution is unitary and the overlap of two wave packets is constant in time. However changing a parameter of the Hamiltonian instead of the initial state will lead to an overlap varying in time. This idea was formulated by Peres [1] when he introduced the fidelity, also known as Loschmidt echo [2]. The fidelity is defined as the overlap of an initial state evolved with slightly different Hamiltonians. This quantity has been used to characterise the stability of quantum states [3]. For classically chaotic systems, the fidelity shows some generic behaviour [3].

Here we study the fidelity in the quasi-integrable regime for which not so many results are established [4–8]. We will do this for one of the best known examples of classically chaotic system: the kicked rotor (KR) [9, 10]. In order to understand the fingerprints of classical chaos in quantum mechanics the quantum kicked rotor (QKR) has been and still is a fruitful field of study [11]. It shows several interesting phenomena like quantum resonance [12] and dynamical localisation [13] both in direct contradiction to the behaviour of the classical system. In the implementation of the QKR near a quantum resonance in the gravity field Oberthaler *et al.* observed quantum accelerator modes [14]. Fishman *et al.* were able to describe these theoretically using a pseudo-classical limit. There the detuning of the kicking period to its resonant value plays the

role of the Planck constant [15]. Using this treatment the QKR can be mapped onto a kicked rotor with a renormalized kicking strength. This leads to regular structures and allows the application of semi-classical methods in the pseudo-classical limit although the system might be chaotic in the true semi-classical limit [16].

The KR shows two types of motion in the quasi-integrable regime, oscillations about the stable fixed points and rotating motion. The motion on the classical resonance island surrounding the fixed point leads to revivals of the quantum fidelity. This was shown for the regular QKR by Sankaranarayanan *et al.* [5] and for the near resonant QKR by Abb *et al.* [6]. Similar results were obtained for another kicked system by Krivolapov *et al.* [7]. Rotational and oscillating orbits were also numerically studied in [8]. Our focus in this paper is to treat the rotating modes of the QKR near a quantum resonance. Therefore we will use the pseudo-classical method and apply the pendulum approximation. Section 2 sets the stage by reviewing the pseudo-classical approximation and defining the fidelity which is studied here. In Section 3 we will give a perturbative treatment of the pendulum and discuss its validity based on a comparison with numerical simulations in Section 4. An additional numerical check is shown in Sect. 5.

## 2. Fidelity for the atom optical kicked rotor

The story of the experimental investigation of the quantum kicked rotor is quite long [17] and it has been continuing until today (see, e.g., the refs. [18–20] and, for fidelity measurements specifically, the refs. [21]). In the experimental realisations, atoms are kicked by a periodic potential formed by a standing wave of laser light, i.e. an optical lattice which is flashed on and off periodically in time [17, 22]. Using rescaled dimensionless momentum  $p$ , position  $x$ , kicking period  $\tau$  and kicking strength  $k$ , see e.g. [15], the Hamiltonian for one kicked atom is:

$$H(p, x, t) = \frac{p^2}{2} + k \cos(x) \sum_{n=-\infty}^{\infty} \delta(t - n\tau). \quad (1)$$

The Floquet operator mapping the state right after one kick to the state right after the next kick is, see e.g. [11],

$$\hat{\mathcal{U}} = e^{-ik \cos(\hat{X})} e^{-i\frac{\tau}{2} \hat{P}^2}. \quad (2)$$

The dynamics is obtained by repeated application of this operator. In contrast to the usual kicked rotor, a kicked atom lives along a line. Doing a gauge transformation one can still recover a problem with conserved quasi-momentum, see e.g. [15, 16]. Here the quasi-momentum corresponds to the fractional part of the momentum  $p = n + \beta$ , where  $n$  is an integer and  $\beta$  is a real variable between 0 and 1. The problem of one atom along a line is mapped onto a problem of a continuous family of rotors. Each of them corresponds to one value of  $\beta$ . That is the reason why we will speak from now on of a  $\beta$ -rotor. In realisations of the kicked rotor with Bose-Einstein condensates it has been checked that the interactions between atoms in the cloud can be neglected [18, 19]. This

brings another justification of our one particle approach. The wave function of a single  $\beta$ -rotor  $|\Psi_\beta\rangle$  is obtained from the wave function of the kicked atom  $|\psi\rangle$  by [15, 16]:

$$\langle\theta|\Psi_\beta\rangle = \frac{1}{\sqrt{2\pi}} \sum_{n \in \mathbb{Z}} \langle n + \beta | \psi \rangle e^{in\theta}, \quad (3)$$

while the Floquet operator for one  $\beta$ -rotor is

$$\hat{\mathcal{U}}_\beta = e^{-ik \cos \hat{\theta}} e^{-i\frac{\tau}{2}(\hat{\mathcal{N}} + \beta)^2}, \quad (4)$$

where  $\hat{\mathcal{N}}$  is the angular momentum operator. The operator (4) formally differs from the usual Floquet operator [11] only by the quasi-momentum  $\beta$ .

A principal quantum resonance occurs in the kicked particle when the phase due to the free evolution in (4) vanishes [23]. Each resonance leads to a ballistic motion and a quadratic growth of the energy. This happens at  $\tau = 2\pi l$  and for resonant quasi-momenta  $\beta_{\text{res}} = 1/2 + q/l$  for integers  $l$  and  $q$  such that  $l \geq 1$  and  $0 \leq q \leq l - 1$ . To simplify the notation, in this paper we consider the specific resonance with  $\tau = 2\pi$  and  $\beta_{\text{res}} = 1/2$ .

Take now a kicking period slightly detuned from its resonant value  $\tau = 2\pi + \epsilon$ . Introducing the rescaled momentum  $\hat{I} = |\epsilon|\hat{\mathcal{N}}$  we can rewrite the Floquet operator (4) as

$$\hat{\mathcal{U}}_{k,\beta} = e^{-\frac{i}{|\epsilon|}\tilde{k} \cos(\hat{\theta})} e^{-\frac{i}{|\epsilon|} \left[ \text{sgn}(\epsilon) \frac{I^2}{2} + \hat{I}(-\pi + \tau\beta) \right]}. \quad (5)$$

This operator can be identified as the formal quantisation of another *fictitious* kicked rotor. The main benefit of this mapping is that the kicking strength of the new problem is  $\tilde{k} = |\epsilon|k$  and  $|\epsilon|$  plays the role of the Planck constant. We will be interested from now on in the regime  $|\epsilon| \rightarrow 0$ , called  $\epsilon$ -semiclassical limit [15], which must not be confused with the *true* semiclassical one of the initial problem. In the  $\epsilon$ -semiclassical limit one can derive easily the  $\epsilon$ -classical map, which is very similar to the celebrated standard map [9]:

$$\begin{aligned} I_{t+1} &= I_t + \tilde{k} \sin(\theta_{t+1}) \\ \theta_{t+1} &= \theta_t + \text{sgn}(\epsilon)I_t - \pi + \tau\beta \pmod{2\pi}. \end{aligned} \quad (6)$$

We are interested in the dynamics around a stable fixed point of (6). One common approximation is the pendulum approximation [9, 10]:

$$H_{\text{Pen}}(I, \theta) = \frac{(I + \xi)^2}{2} + \tilde{k} \cos \theta, \quad (7)$$

where we have defined  $\xi = \text{sgn}(\epsilon)(-\pi + \tau\beta)$ . For a given (even large) kicking strength  $k$ , one can always choose a small enough  $\epsilon$  so that we are in the quasi-integrable regime. This makes the phase spaces corresponding to (6) and (7), respectively, very similar, see Fig. 1.

The main goal of this paper is to check the stability of the quantum dynamics under slight variation of the kicking strength. The fidelity [1, 3] appears as the natural quantity to look at. For one single  $\beta$ -rotor it is defined as:

$$F_\beta(k_1, k_2, t) = \left| \langle \psi_0 | \mathcal{U}_{k_1, \beta}^t \dagger \mathcal{U}_{k_2, \beta}^t | \psi_0 \rangle \right|^2. \quad (8)$$

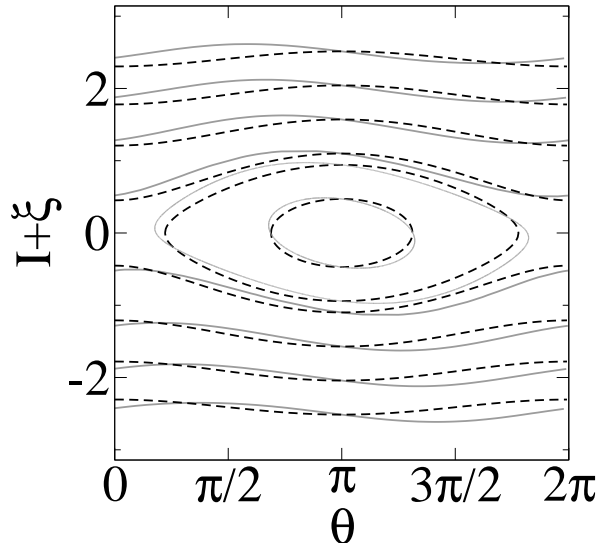


**Figure 1.** (Colour online) Phasespace of the pendulum (black - - -) and the kicked rotor (grey —) for  $\tilde{k} = |\epsilon|k = 0.08\pi$ .

For the initial problem of a kicked atom one needs to consider the fidelity for a sub-ensemble of rotors, which is defined then by [24, 25]:

$$F(k_1, k_2, \beta_1, \Delta\beta, t) = \left| \int_{\beta_1}^{\beta_1 + \Delta\beta} d\beta \langle \psi_0 | \mathcal{U}_{k_1, \beta}^t \dagger \mathcal{U}_{k_2, \beta}^t | \psi_0 \rangle \right|^2. \quad (9)$$

If the initial state mainly lives on the stable island the fidelity shows revivals as explained in [6], see also a similar context in [7]. Here the study will be devoted to the fidelity (8) in the neighbourhood of such an island. We will approximate (8) by the fidelity of the pendulum (7). The fidelity of the pendulum is obtained by expanding the initial state in the eigenbasis  $|\phi_n(k)\rangle$  of the Hamiltonian $\ddagger$  of Eq. (7), which depends on  $\beta$  via  $\xi$ .

$$F_\beta(k_1, k_2, t) = \left| \sum_{n,m} \langle \Psi_\beta(t=0) | \phi_n(k_2) \rangle \langle \phi_n(k_2) | \phi_m(k_1) \rangle \langle \phi_m(k_1) | \Psi_\beta(t=0) \rangle e^{i \frac{t}{|\epsilon|} (E_n^{k_2} - E_m^{k_1})} \right|^2. \quad (10)$$

Throughout the paper we focus on the quantum problem associated to (5) so that  $|\epsilon|$  is always our Planck constant. This is the reason why we will call the  $\epsilon$ -semiclassical regime simply the semiclassical regime.

### 3. Perturbative treatment of the pendulum

We are interested in the quantum pendulum following the approximation (7). It is well known that this system is quantum mechanically integrable [26]. Following (10) we want to obtain simple explicit formulæ for the eigenenergies  $E_n^k$  and the eigenfunctions  $|\phi_n(k)\rangle$  of the Hamiltonian when  $|\epsilon|$  is going to 0. We will follow standard perturbation

$\ddagger$  We emphasise the dependence of the eigenstates on  $k$  as it is the perturbation parameter in the fidelity.

theory. The only unusual thing is that the potential is proportional to the effective Planck constant so that it vanishes at the classical limit  $|\epsilon| = 0$ .

Our unperturbed system is a free particle along a ring with eigenenergy and eigenfunction ( $m \in \mathbb{Z}$ ):

$$E_m = \frac{(m|\epsilon| + \xi)^2}{2} = \frac{\xi^2}{2} + \xi m|\epsilon| + \mathcal{O}(|\epsilon|^2), \quad (11)$$

$$\langle \theta | \phi_m \rangle = \frac{e^{im\theta}}{\sqrt{2\pi}}. \quad (12)$$

For  $\tilde{k} > 0$  the Schrödinger equation for the stationary states becomes:

$$\frac{1}{2} \left( -i|\epsilon| \frac{\partial}{\partial \theta} + \xi \right)^2 \Psi + \tilde{k} \cos \theta \Psi = E \Psi. \quad (13)$$

Doing the gauge transformation  $\Psi = \exp(-i\xi\theta/|\epsilon|)\psi$  and setting  $\psi(\theta) = f(z = \theta/2)$ , Eq. (13) becomes:

$$\frac{d^2 f}{dz^2} + \left( \frac{8E}{|\epsilon|^2} - 2 \frac{4\tilde{k}}{|\epsilon|^2} \cos(2z) \right) f(z) = 0, \quad (14)$$

which is the standard form of Mathieu equation, see e.g. 16.2.1 p.97 in [27]. For our purpose it is easier to look for a solution of (14) as the following series:

$$f(z) = \sum_{n \in \mathbb{Z}} c_n e^{(\mu + 2in)z}. \quad (15)$$

As we require the “true” wave function  $\Psi(\theta)$  to be univalued one can easily see that we need

$$\mu = \frac{2i\xi}{|\epsilon|}. \quad (16)$$

The eigenenergies of (13) are given by characteristic values of Mathieu functions, which do not lead to simple explicit formulæ. A semiclassical approach is rather used to write an expansion of the eigenenergies. The details are found in the Appendix A. The results are, assuming  $\tilde{k} = k|\epsilon|$  and noting  $\xi_0 = \text{sgn}(\epsilon)\pi(2\beta - 1)$ :

$$\begin{aligned} E_m^k \simeq & \frac{\xi_0^2}{2} + \xi_0(m + \beta)|\epsilon| + \left( \frac{(m + \beta)^2}{2} + \frac{k^2}{4\xi_0^2} \right) |\epsilon|^2 - \frac{(m + \beta)k^2}{2\xi_0^3} |\epsilon|^3 \\ & + \left( \frac{3(m + \beta)^2 k^2}{4\xi_0^4} + \frac{5k^4}{64\xi_0^6} \right) |\epsilon|^4. \end{aligned} \quad (17)$$

In (15) the coefficients  $c_n$  are the solutions of the following recurrence relation:

$$[2E - (n|\epsilon| + \xi)^2] c_n = \tilde{k}(c_{n-1} + c_{n+1}). \quad (18)$$

If we assume now that we start from an unperturbed state (12) with the energy (11), (18) can be rewritten as:

$$2 \frac{(n - m)\xi_0}{-k} c_n^{(m)} = c_{n-1}^{(m)} + c_{n+1}^{(m)}, \quad (19)$$

which gives the solution:  $c_n^{(m)} = J_{n-m}(-k/\xi_0)$  where  $J_n(x)$  stands for the Bessel function of integer order  $n$ . The perturbed eigenfunctions are then:

$$\langle \theta | \phi_m(k) \rangle = \sum_{n \in \mathbb{Z}} J_{n-m} \left( \frac{-k}{\xi_0} \right) e^{in\theta} = e^{im\theta - ik \sin(\theta)/\xi_0} \quad (20)$$

where we have used in the second equality the following identity for the Bessel functions, see e.g. 7.2.4(26) p.7 in [28]:

$$\sum_{n \in \mathbb{Z}} J_n(x) e^{in\theta} = e^{ix \sin \theta} . \quad (21)$$

The great benefit from (20) is that we can directly compute the overlap coefficient for the fidelity (10). We assume that the initial state is a plane wave with momentum  $n_0$ :  $\langle n | \Psi_\beta(t=0) \rangle = \delta_{n,n_0}$  where  $\delta_{n,k}$  is the Kronecker symbol. Then:

$$\begin{aligned} \langle \phi_m(k) | \Psi_\beta(t=0) \rangle &= \sum_{n \in \mathbb{Z}} \langle \phi_m(k) | n \rangle \langle n | \Psi_\beta(t=0) \rangle = J_{n_0-m} \left( \frac{-k}{\xi_0} \right) , \quad (22) \\ \langle \phi_m(k_1) | \phi_n(k_2) \rangle &= \sum_{p \in \mathbb{Z}} \langle \phi_m(k_1) | p \rangle \langle p | \phi_n(k_2) \rangle \\ &= J_{m-n} \left( -\frac{k_2 - k_1}{\xi_0} \right) . \quad (23) \end{aligned}$$

Finally our simple perturbative approach lets us write an explicit formula for the fidelity, reminding  $\xi_0 = \text{sgn}(\epsilon)\pi(2\beta - 1)$ :

$$\begin{aligned} F_\beta(k_1, k_2, t) &= \\ & \left| \sum_{n,m \in \mathbb{Z}} J_{m-n} \left( \frac{k_1 - k_2}{\xi_0} \right) J_{n_0-m} \left( \frac{-k_1}{\xi_0} \right) J_{n_0-n} \left( \frac{-k_2}{\xi_0} \right) e^{i \frac{t}{|\epsilon|} (E_n^{k_2} - E_m^{k_1})} \right|^2 , \quad (24) \end{aligned}$$

where  $E_m^{k_1}$  and  $E_n^{k_2}$  are given by (17). The formula (24) is the main result of this paper. In the next section we will estimate numerically the range of validity and the accuracy of (24) to describe the quantum kicked rotor. In Fig. 2 we can already see that the more orders we take for the energy, the more accurate we get.

#### 4. Numerical comparison of the approaches

The perturbative approach, cf. Eq. (24), will now be checked numerically in this section. As single rotors and ensembles show qualitatively different behaviour we treat these cases separately.

Before showing the main results, we discuss the intrinsic limitations of our approach. The phase space of the pendulum is the cylinder whereas the phase space of the KR can be mapped onto a torus. The pendulum approximation is therefore only valid in one phase space cell of the KR. Due to this mismatch we expect the approximation to fail at the border of a cell.

In the derivation of the perturbative result we explicitly focused on the rotating regime, which means that our results have to fail in the description of states on the

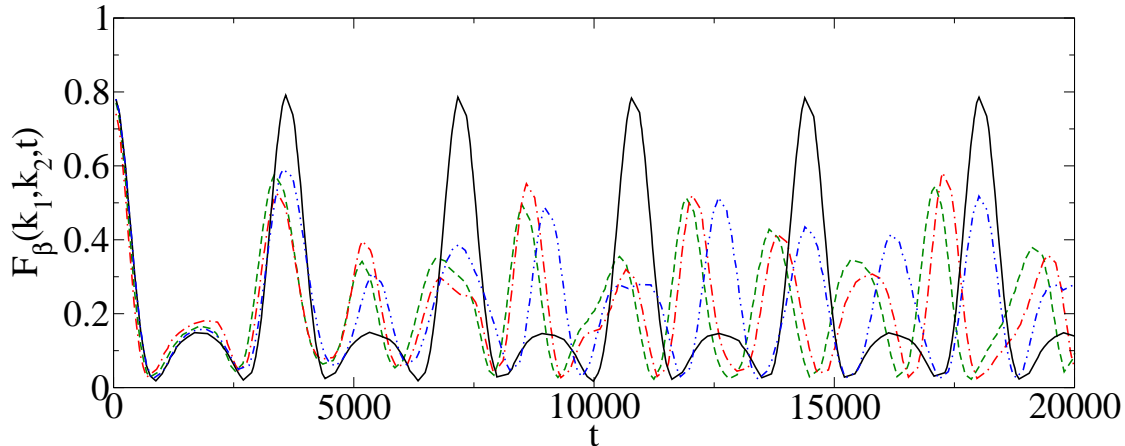


**Figure 2.** (Colour online) Fidelity using the pendulum (green - - -), the perturbative result with the third (black —) and fourth (blue — · · —) order in  $|\epsilon|$  in the energy, and the original QKR (red — · · —).  $\beta = 0.3$ ,  $\epsilon = 0.05$ ,  $k_1 = 0.6\pi$  and  $k_2 = 0.8\pi$ . The data are averaged over 100 kicks in order to cancel fast oscillations.

island. The half width of the island in the pendulum approximation is given by  $\Delta I = 2\sqrt{k|\epsilon|}$  [10], which becomes in units of the quasi-momentum

$$\Delta\beta_c^{\text{th}} = \frac{\Delta I}{\tau} \approx \sqrt{\frac{|\epsilon|k}{\pi^2}}. \quad (25)$$

When the distance from  $\beta$  to its resonant value (centred at the island) is less than  $\Delta\beta_c$  we expect to observe the revivals in the fidelity as described in [6].

#### 4.1. Single rotors

The most important goal of the discussion of single rotors is to get an intuition for the quality of the pendulum approximation. We can discuss this step only for single rotors as the calculation of the pendulum fidelity is numerically very challenging. Averaging the fidelity over 100 kicks allows to identify maxima in the two cases and to read of the amplitude and the period (c.f., for instance, Fig. 3). Plotting the relative deviation of the period of the maxima one observes that this relative error is nearly independent of the choice of the maximum. As a measure of deviation of the amplitude we compared a limited number of maxima, whilst these maxima should be visible both in the QKR and the pendulum data. We decide to take the maximal deviation within the first 10 maxima.

When requiring an accuracy of 10% we can give as a boundary of validity  $\beta \gtrsim 0.2$ . In the case of the amplitude the criterion is not as clear. Taking also the deviation in the amplitude into account we concluded that  $\beta \gtrsim 0.3$  following this criterion.

#### 4.2. Ensembles

In order to build ensembles we need to evaluate the integral in (9). This integral is approximated by a Riemann sum with  $N_\beta$  values of  $\beta$  uniformly distributed in

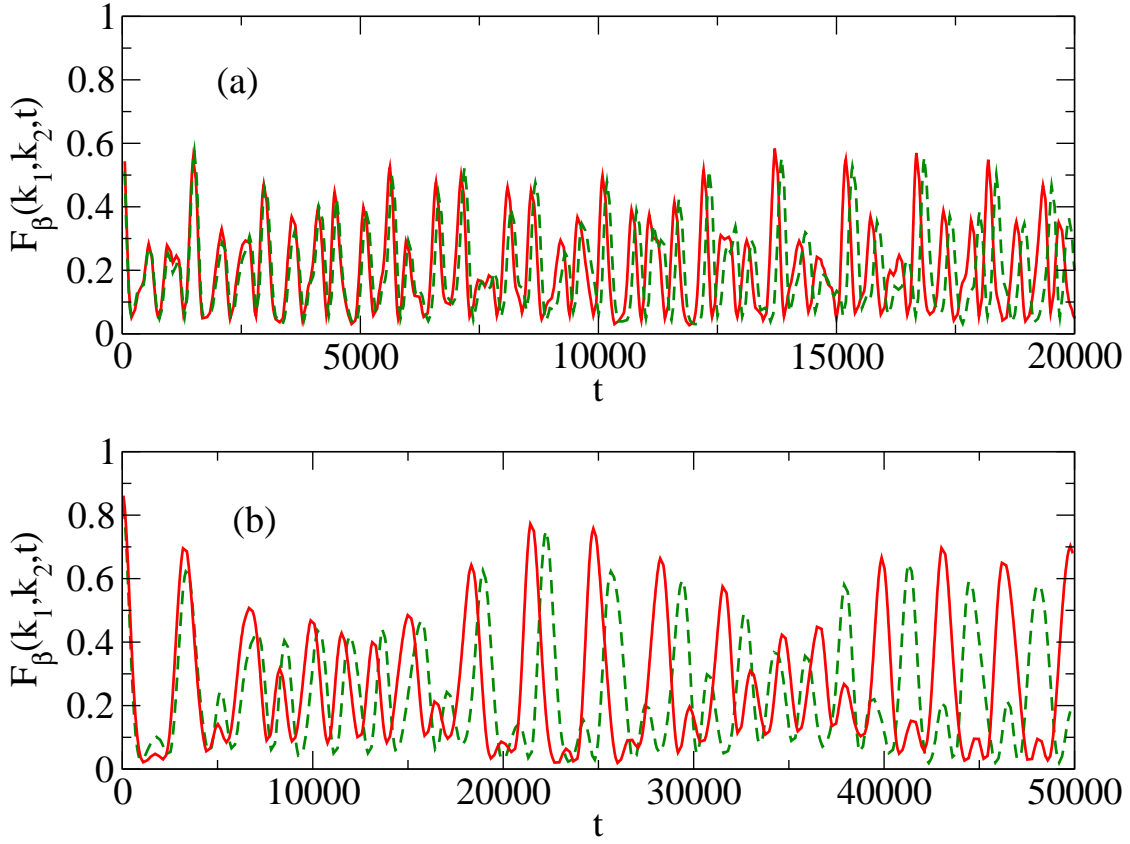


**Figure 3.** (Colour online) Fidelity for the QKR (red —) and the pendulum (green - - -) for  $\epsilon = 0.075$ ,  $k_1 = 0.6\pi$  and  $k_2 = 0.8\pi$ . (a)  $\beta = 0.3216$ , (b)  $\beta = 0.2412$ . The data are averaged over 100 kicks in order to get rid of the fast oscillations.

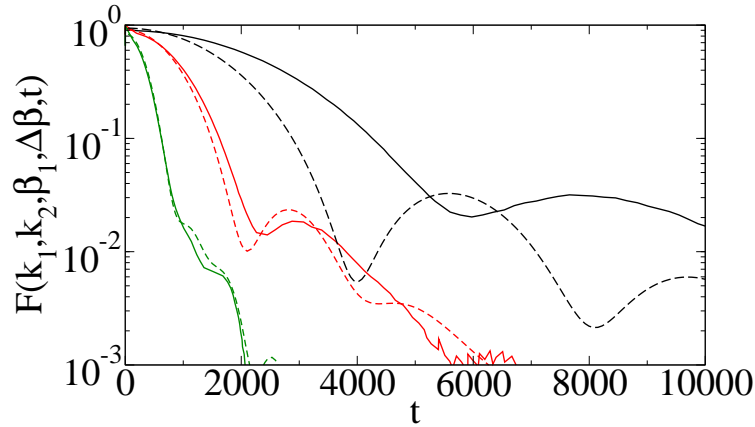


**Figure 4.** (Colour online) Comparison between the fidelity for the perturbative approach (dashed line) and the QKR (solid line),  $\epsilon = 0.05$ ,  $k_1 = 0.6\pi$ ,  $k_2 = 0.8\pi$ ,  $\Delta\beta = 0.06$ ,  $\beta_1 = 0.06$  (black, right),  $\beta_1 = 0.14$  (red, middle),  $\beta_1 = 0.22$  (green, left).

$[\beta_1, \beta_1 + \Delta\beta]$ . It has been checked that  $N_\beta$  should be of order of a few thousand to get a reasonably good approximation for the integral in (9).

For the boundary of the phase space cell the same criterion as used for single rotors



| $\epsilon$ | range for ensemble                             | theoretical upper bound |
|------------|--|-------------------------|
| 0.1        | $0.10 - 0.16 < \beta_1, \beta_2 < 0.36 - 0.37$ | 0.34                    |
| 0.05       | $0.12 - 0.16 < \beta_1, \beta_2 < 0.39 - 0.41$ | 0.39                    |
| 0.01       | $0.12 - 0.16 < \beta_1, \beta_2 < 0.45 - 0.47$ | 0.45                    |

**Table 1.** Range of validity of the pendulum approximation. For simplicity we defined  $\beta_2 = \Delta\beta + \beta_1$ .

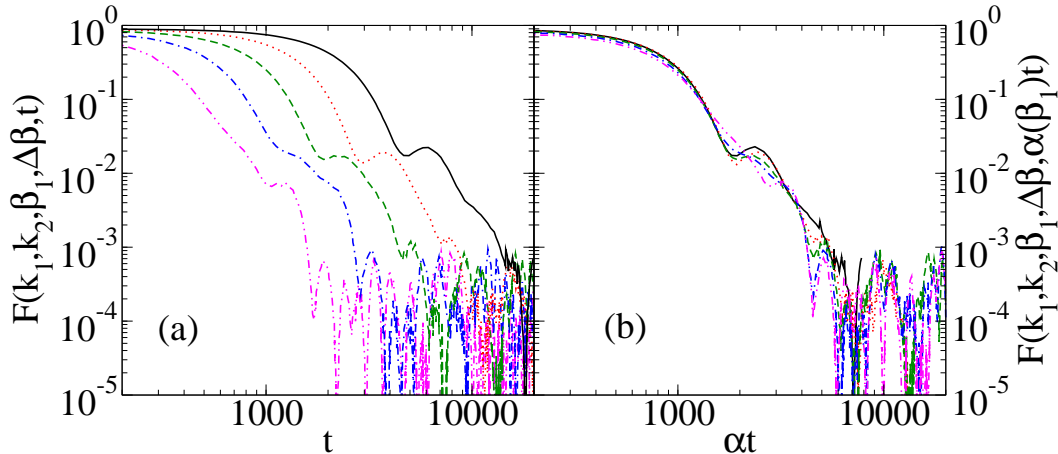


**Figure 5.** (Colour online) Fidelity of a few ensembles of  $\beta$ -rotors with  $\epsilon = 0.05$ ,  $\Delta\beta = 0.06$ ,  $k_1 = 0.6\pi$ ,  $k_2 = 0.8\pi$ ,  $\beta_1 = 0.08$  (black —),  $\beta_1 = 0.12$  (red ·····),  $\beta_1 = 0.16$  (green - - - -),  $\beta_1 = 0.2$  (blue — · —) and  $\beta_1 = 0.24$  (magenta — · · —). In (a) the original data and in (b) the rescaled data are shown. The scaling factors are according to figure 6.

is applied. In Fig. 4 a few ensembles are shown. For the measure of correspondence we compare the widths of the first few pseudo-oscillations and also demand a deviation of less than 10% here. The onset of the island behaviour near to a resonance leads to small peaks in the fidelity as described in [6]. Therefore the occurrence of these peaks defines the critical value near the resonance island. The intervals for several  $\epsilon$  are summarised in Table 1. The upper bound is described quite well by the estimate due to the pendulum approximation (25) and only fails for the largest  $\epsilon$  presented, i.e. far from the semiclassical regime.

## 5. Scaling of ensembles

In this section we perform additional numerical analysis over a larger range of parameters. This will confirm the range of validity of our perturbative approach.

The ensembles in Fig. 5a show a similar fidelity as a function of time except for a shift along the time axis. This suggests a rescaling of the time. First choose a reference value of  $\beta$ , say  $\beta_{\text{ref}}$ . Then we claim that we can map the fidelity for *another*  $\beta_1$  on top of the reference value only by rescaling the time. This can be more formally written in

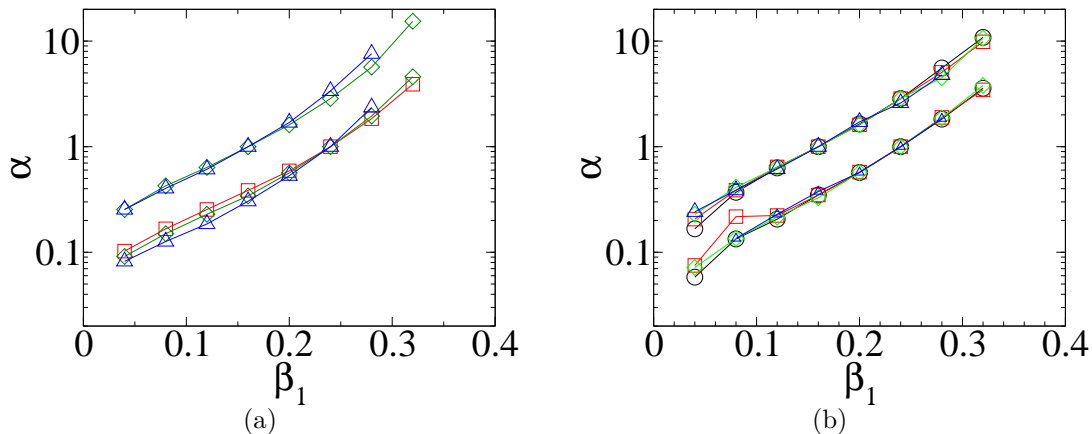


**Figure 6.** (Colour online) Scaling factors for several parameters. The scaling is done for two references  $\beta_{\text{ref}} = 0.16$  (upper curves) and  $\beta_{\text{ref}} = 0.24$  (lower curves).  $k_2 = 0.8\pi$ ,  $\Delta\beta = 0.03$  (black circles),  $\Delta\beta = 0.06$  (red squares),  $\Delta\beta = 0.09$  (green diamonds),  $\Delta\beta = 0.12$  (blue triangles). (a)  $\epsilon = 0.005$   $\Delta k = 0.2\pi$ , and (b)  $\epsilon = 0.05$   $\Delta k = 0.1\pi$ .

the following way ( $\beta_{\text{ref}}$  is chosen a priori):

$$F(k_1, k_2, \beta_1, \Delta\beta, t) \approx F(k_1, k_2, \beta_{\text{ref}}, \Delta\beta, \alpha(\beta_1)^{-1} t). \quad (26)$$

The fidelity is scaled such that a box surrounding the mean decay can be kept as narrow as possible. An example where the curves in Fig. 5a have been rescaled is presented in Fig. 5b. One may notice that the formula (26) comes from heuristic and numerical observations. It is believed to work as long as the pendulum approximation does for the kicked rotor. The latter approximation cannot be controlled in a simple way [9]. That is the reason why we will only give here numerical bounds for the validity of (26).

This scaling procedure was done for several  $\beta_1$ ,  $\Delta\beta$ ,  $\epsilon$  and  $k_1$ , whereas  $k_2$  was kept the same. The procedure was repeated for another reference  $\beta_{\text{ref}}$ . We expect the curves corresponding to different reference values to be parallel, i.e. a different choice of  $\beta_{\text{ref}}$  just leads to a constant offset. The resulting plots are presented in Fig. 6. We can see that the scaling factor has no strong dependence on any of the parameters shown.

The same scaling procedure also has been performed for the perturbative data computed from (24). In Fig. 7 we show the comparison between scaling factors of the perturbative result and the QKR for one set of parameters. We observe a reasonable agreement. Below  $\beta_1 \approx 0.12$  there is a systematical deviation between Eq. (24) and the QKR data. This corresponds to the border of the phase space cell where we already expect the pendulum approach to fail. One may conclude that the rescaling procedure is valid as long as the pendulum approximation holds. More precisely in our case the range of validity is given by the numerical bounds stated above in Sect. 4.2.

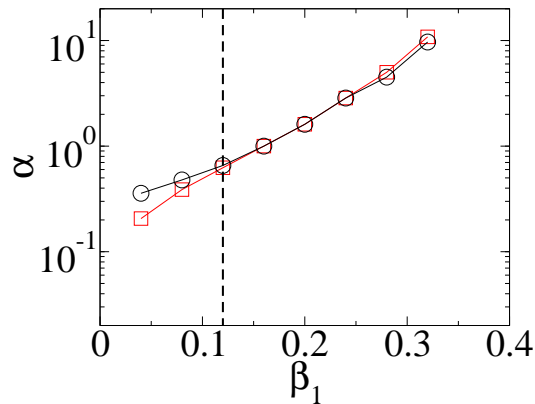


**Figure 7.** (Colour online) Scaling factors for the perturbative result (black circles) and QKR data (red squares), for  $\epsilon = 0.05$ ,  $k_1 = 0.6\pi$ ,  $k_2 = 0.8\pi$ ,  $\beta_{\text{ref}} = 0.16$  and  $\Delta\beta = 0.06$ . The dashed line is the border of correspondence between the QKR and the perturbative result given in Table 1.

## 6. Summary and outlook

We have for the first time studied analytically the quantum fidelity of initial conditions corresponding to rotational orbits in the underlying pseudo-classical model. Using the pendulum approximation for these orbits, we arrive at our main analytical result summarised in Eq. (24). Although we use a formally somewhat inconsistent expansion in the perturbation parameter  $\epsilon$ , we see that our approximation is rather good when including higher orders in the dynamical phases, even if just the lowest order in the amplitude of the wave functions is considered. We give clear ranges of applicability of our approximation which were tested against numerical simulations of the original quantum kicked rotor system. Within these ranges a scaling hypothesis for the temporal decay of the fidelity is found which is fulfilled by the original model as well as our perturbative results. It would be interesting to set this scaling hypothesis onto firm grounds by deriving it from first principles for the here investigated rotational pseudo-classical orbits. This task is left for future investigations.

## Acknowledgments

It is our great pleasure to thank Italo Guarneri for illuminating discussions at the early stage of this work. This work was supported by the DFG through FOR760, the Helmholtz Alliance Program of the Helmholtz Association (contract HA-216 Extremes of Density and Temperature: Cosmic Matter in the Laboratory), and within the framework of the Excellence Initiative through the Heidelberg Graduate School of Fundamental Physics (grant number GSC 129/1), the Frontier Innovation Fund and the Global Networks Mobility Measures.

## Appendix A. Perturbative expansion of the pendulum energy levels

We are interested in the quantum energy levels of the pendulum Hamiltonian (7). It is worth reminding that  $\tilde{k} = k|\epsilon|$  where  $|\epsilon|$  is our effective Planck constant. We are interested in the regime of small  $|\epsilon|$ . Our procedure is the following: assume first that  $|\epsilon|$  is a fixed small quantity. Then write perturbative expansions in  $\tilde{k}$ , which are valid whenever  $\tilde{k} = \mathcal{O}(|\epsilon|)$ . At the very end we will write more explicitly  $\tilde{k} = k|\epsilon|$  to derive  $\epsilon$ -semiclassical results.

The classical action for the Hamiltonian (7) along a trajectory from  $\theta_i$  to  $\theta$  at a fixed energy  $E$  is:

$$S(\theta, \theta_i) = \int_{\theta_i}^{\theta} \sqrt{2(E - \tilde{k} \cos \varphi)} d\varphi - \xi(\theta - \theta_i) , \quad (\text{A.1})$$

where  $\xi = \text{sgn}(\epsilon)(-\pi + \tau\beta) = \xi_0 + |\epsilon|\beta$ . The energy level can be well described using a WKB-like approach in the regime  $|\epsilon| \rightarrow 0$  by:

$$\int_0^{2\pi} \sqrt{2(E_m^k - \tilde{k} \cos \varphi)} d\varphi - 2\xi\pi = 2\pi m|\epsilon| . \quad (\text{A.2})$$

Here the Maslov index is 0 as the particle lives on a ring, hence never meets any boundary. The quantization condition (A.2) with integers  $m$  can be rewritten in a more efficient way as

$$4\sqrt{2(E_m^k - \tilde{k})} \mathbb{E} \left( i\sqrt{\frac{2\tilde{k}}{E_m^k - \tilde{k}}} \right) = 2\pi [(m + \beta)|\epsilon| + \xi_0] , \quad (\text{A.3})$$

where  $\mathbb{E}(\kappa)$  is the Legendre complete elliptic integral:

$$\mathbb{E}(\kappa) = \int_0^{\pi/2} \sqrt{1 - \kappa^2 \sin^2(t)} dt . \quad (\text{A.4})$$

Eq. (A.3) is the starting point of our perturbation expansion. We assume from now that  $\xi \neq 0$ . For the left hand side of (A.3) the Taylor expansion of  $\mathbb{E}(\kappa)$  is used, see e.g. 8.114 (1) p.853 in [29]:

$$\mathbb{E}(\kappa) = \frac{\pi}{2} \left[ 1 - \frac{\kappa^2}{4} - \frac{3\kappa^4}{64} - \frac{5\kappa^6}{256} - \frac{175\kappa^8}{16384} + \mathcal{O}(\kappa^{10}) \right] \quad (\text{A.5})$$

One gets:

$$\begin{aligned} \mathbb{E} \left( i\sqrt{\frac{2\tilde{k}}{E_m^k - \tilde{k}}} \right) = \\ \frac{\pi}{2} \left[ 1 + \frac{\tilde{k}}{2E_m^k} + \frac{5\tilde{k}^2}{16E_m^{k2}} + \frac{9\tilde{k}^3}{32E_m^{k3}} + \frac{241\tilde{k}^4}{1024E_m^{k4}} + \mathcal{O} \left( \frac{\tilde{k}^5}{E_m^{k5}} \right) \right] \end{aligned} \quad (\text{A.6})$$

The eigenenergy  $E_m^k$  is assumed to have the following form:

$$E_m^k = \frac{\xi_0^2}{2} + \xi_0(m + \beta)|\epsilon| + \alpha_2\epsilon^2 + \alpha_3|\epsilon|^3 + \alpha_4\epsilon^4 \quad (\text{A.7})$$

Identifying both parts of (A.3) using (A.6) leads to the following results:

$$\alpha_2 = \frac{(m + \beta)^2}{2} + \frac{k^2}{4\xi_0^2} \quad (\text{A.8})$$

$$\alpha_3 = -\frac{(m + \beta)k^2}{2\xi_0^3} \quad (\text{A.9})$$

$$\alpha_4 = \frac{3}{4} \frac{(m + \beta)^2 k^2}{\xi_0^4} + \frac{5}{64} \frac{k^4}{\xi_0^6} \quad (\text{A.10})$$

Inserting (A.8), (A.9) and (A.10) into (A.7) gives (17).

- [1] Peres A 1984 *Phys. Rev. A.* **30** 1610
- [2] Jalabert RA and Pastawski HM 2001 *Phys. Rev. Lett.* **86** 2490
- [3] Gorin T, Prosen T, Seligman T H and Znidaric M *Physics Reports* **435** 33 - 156  
Jacquod P and Petitjean C 2009 *Adv. Phys.* **58** 67–196
- [4] Benenti G, Casati G and Veble G 2003 *Phys. Rev. E* **68** 036212
- [5] Sankaranarayanan R and Lakshminarayan A 2003 *Phys. Rev. E* **68** 036216
- [6] Abb M, Guarneri I and Wimberger S 2009 *Phys. Rev. E* **80** 035206
- [7] Krivolapov Y, Fishman S, Ott E and Antonsen T M 2011 *Phys. Rev. E* **83** 016204
- [8] Weinstein Y S and Hellberg C S 2005 *Phys. Rev. E* **71** 016209
- [9] Chirikov B V 1979 *Phys. Rep.* **52** 263–379
- [10] Lichtenberg A J and Leiberman M A 1992 *Regular and chaotic dynamics (2nd edition) (Applied Mathematical Sciences vol. 38)* (New York, Springer)
- [11] Izrailev F M 1990 *Phys. Rep.* **196** 299–392
- [12] Izrailev F M and Shepelyanskii D L 1979 *Sov. Phys. Dokl.* **24** 996 (in Russian) transl. in 1980 *Theoretical and Mathematical Physics* **43**, 553-561
- [13] Fishman S, Grepel D R, and Prange R E 1982 *Phys. Rev. Lett.* **49** 509-512
- [14] Oberthaler M K, Godun R M, d’Arcy M B, Summy G S and Burnett K 1999 *Phys. Rev. Lett.* **83** 4447-4451
- [15] Fishman S, Guarneri I and Rebuzzini L 2003 *J. Stat. Phys.* **110** 911–943
- [16] Wimberger S, Guarneri I and Fishman S 2003 *Nonlinearity* **16** 1381
- [17] Moore F L, Robinson J C, Bharucha C F, Sundaram B and Raizen M G 1995 *Phys. Rev. Lett.* **75** 4598–4601
- [18] Wimberger S, Mannella R, Morsch O and Arimondo E 2005 *Phys. Rev. Lett.* **94** 130404  
Rebuzzini L, Artuso R, Fishman S and Guarneri I 2007 *Phys. Rev. A* **76** 031603(R)
- [19] Ryu C, Andersen MF, Vaziri A, d’Arcy MB, Grossman JM, Helmersson K and Phillips WD 2006 *Phys. Rev. Lett.* **96** 160403  
Talukdar I, Shrestha R, and Summy G S 2010 *Phys. Rev. Lett.* **105** 054103
- [20] d’Arcy MB, Godun RM, Oberthaler MK, Cassettari D and Summy GS 2001 *Phys. Rev. Lett.* **87** 074102  
d’Arcy MB, Godun RM, Summy GS, Guarneri I, Wimberger S, Fishman S and Buchleitner A 2004 *Phys. Rev. E* **69** 027201  
Wimberger S, Sadgrove M, Parkins S and Leonhardt R 2005 *Phys. Rev. A* **71** 053404  
Kanem JF, Maneshi S, Partlow M, Spanner M and Steinberg AM 2007 *Phys. Rev. Lett.* **98** 083004  
Lemarié G, Lignier H, Delande D, Szriftgiser P and Garreau J C 2010 *Phys. Rev. Lett.* **105** 090601
- [21] Schlunk S, d’Arcy MB, Gardiner SA and Summy GS 2003 *Phys. Rev. Lett.* **90** 054101  
Wu S, Tonyushkin A and Prentiss MG 2009 *Phys. Rev. Lett.* **103** 034101
- [22] Graham R, Schlautmann M and Zoller P 1992 *Phys. Rev. A* **45** R19
- [23] Izrailev F M 1986 *Phys. Rev. Lett.* **56** 541–544
- [24] Buchleitner A and Wimberger S 2006 *J. Phys. B: At. Mol. Opt. Phys.* **39** L145–L151

- [25] Wimberger S 2004 *PhD Thesis* Ludwig-Maximilians-Universität Munich/Università degli Studi dell'Insubria (<http://edoc.ub.uni-muenchen.de/archive/00001687>)
- [26] Condon E U 1928 *Phys. Rev.* **31** 891-894
- [27] Erdelyi A et al 1953 *Higher transcendental functions* vol. 3 (New York, Mc-Graw-Hill)
- [28] Erdelyi A et al 1953 *Higher transcendental functions* vol. 2 (New York, Mc-Graw-Hill)
- [29] Gradshteyn I S, Ryzhik I M 2000 *Table of Integrals, Series and Products (6th edition)* (San Diego, Acad. Press)